Hindawi Publishing Corporation
Journal of Nanomaterials
Volume 2007, Article ID 30389, 9 pages
doi:10.1155/2007/30389

Review Article

The AC and DC Conductivity of Nanocomposites

David S. McLachlan[1,2] and Godfrey Sauti[1,3]

[1] *Department of Chemistry and Polymer Science, University of Stellenbosch, Private Bag X1, Matieland 7602, South Africa*
[2] *Materials Physics Research Institute, School of Physics, University of the Witwatersrand, Private Bag 3, Wits 2050, South Africa*
[3] *National Institute of Aerospace, 100 Exploration Way, Hampton, VA 23666, USA*

Received 25 April 2007; Accepted 9 August 2007

Recommended by Christian Brosseau

The microstructures of binary (conductor-insulator) composites, containing nanoparticles, will usually have one of two basic structures. The first is the matrix structure where the nanoparticles (granules) are embedded in and always coated by the matrix material and there are no particle-particle contacts. The AC and DC conductivity of this microstructure is usually described by the Maxwell-Wagner/Hashin-Shtrikman or Bricklayer model. The second is a percolation structure, which can be thought to be made up by randomly packing the two types of granules (not necessarily the same size) together. In percolation systems, there exits a critical volume fraction below which the electrical properties are dominated by the insulating component and above which the conducting component dominates. Such percolation systems are best analyzed using the two-exponent phenomenological percolation equation (TEPPE). This paper discusses all of the above and addresses the problem of how to distinguish among the microstructures using electrical measurements.

1. INTRODUCTION

As it is all but impossible to measure the electrical properties of a single particle, which is three-dimensionally a nanoparticle, its electrical properties will usually have to be deduced from a compact or a composite containing the nanoparticles. A measurement of the electrical properties is also important as it is usually not possible to deduce the connectivity of a composite system from SEM and TEM micrographs alone. This paper will show how to analyze the AC and DC conductivity, or complex dielectric constant, of binary (conductor and insulator) nanocomposites (media, compacts). Most binary and some tertiary media (with some ingenuity, the analysis can be applied to tertiary media), which are found in practice to at least approximate one of the two basic nanostructures, are discussed in this paper. The first are matrix media, where the matrix phase surrounds the granular (particle) phase at all volume fractions and the distance between the conducting particles is greater than the tunneling distance for electrons. This is usually best described using the Maxwell-Wagner effective media equation (also known as the Maxwell-Garnet equation). The Maxwell-Wagner model is formally equivalent to the Hashin-Shtrikman [1] lower bound (insulator host) and upper bound (conductor host) [2, 3] and will be referred to here as the Maxwell-Wagner/Hashin-Shtrikman (MW/HS) model. For matrix dominated media, the Bricklayer model (BLM) [4] is also useful. The second nanostructure is where the conducting particles, in a two-phase material, make electrical contact with each other, when the volume fraction of the conducting particles φ reaches a certain critical φ_c. At this point, a critical or spanning cluster is formed and there is an abrupt (usually many orders of magnitude) change in the DC conductivity. The complex electrical conductivity of these systems is best [5, 6] described by the two-exponent phenomenological percolation equation (TEPPE) (also known as the general effective medium (GEM) equation) [7–17]. The three standard percolation equations are reviewed by Clerc et al. [18], Bergman and Stroud [19], and Nan [20], but it is specifically shown by McLachlan et al. [5, 6] that, while the single TEPPE reduces to the three standard equations in the appropriate limits, it is far superior in the second-order terms (i.e., the imaginary dielectric constant ε_{mi} in the conducting media above φ_c and the dielectric loss ε_{ii} (or σ_{mr}) below φ_c). The theory given here applies to nano-, micro-, and macromedia. Note that the word nanostructure is used throughout this paper although most of the existing experimental results are for microstructures. Section 2.1 deals with

the MW/HS equations, the specific nano- (micro-) structure pertaining to the MW/HS equations [2, 21], as well as observations regarding its applicability to nanostructures. The "rectangular" Bricklayer model [4], widely used in microceramics, which could be appropriate for rectilinear nanostructures, is not discussed in this paper. Section 2.2 describes percolation media and some of the nanostructures which give rise to φ_c's between 0.0005 [22] and 0.56 [23]. The TEPPE, which is widely used to describe percolation systems, is introduced in Section 2.3. This section is widely illustrated by experimental results. Section 2.4 gives a brief discussion of what features in the nanostructure determine the values of the percolation exponents, s and t, as well as discussing charging effects. Ways of differentiating between effective media and percolation media are discussed in Section 3.

2. THEORY AND RESULTS

The AC conductivity of the media (composites) (σ_m) is the sum of the real and imaginary conductivities, which is given by $\sigma_m = \sigma_{mr} + i\sigma_{mi}$. The conductivity of the more conducting component is given by $\sigma_c = \sigma_{cr} + i\sigma_{ci}$ or simply $\sigma_c = \sigma_{cr}$ if ideal conductivity ($\sigma_{cr} \gg \sigma_{ci}$) is assumed. For the insulating component, the conductivity is $\sigma_i = \sigma_{ir} + i\sigma_{ii}$, where $\sigma_{ii} = \omega\varepsilon_0\varepsilon_{ir}$. σ_i is often approximated as $\sigma_i = i\omega\varepsilon_0\varepsilon_{ir}$ (i.e, $\sigma_{ir} \ll i\sigma_{ii}$). In practice, σ_{ir} incorporates both, a usually very small, DC conductivity and the dielectric polarization loss term ($\omega\varepsilon_0\varepsilon_{ii}$). The expressions for σ_c and σ_i can be dispersive and/or temperature-dependant. Although, to the best of the authors' knowledge, it has never been attempted for an experimental system, Nan [20] showed how a granular component can be modeled as consisting of both a core and a coating. The theory given in this paper definitely applies to micro- and macromedia and most nanostructures, but there are some special features regarding nanostructures which must be considered. In nanostructures, the coating matrix component thickness and the interparticle distances will often be 10 nm thick or less. From 10 nm or less, the coatings are below the tunneling distance for electrons, which would mean that the bulk conductivity (σ_{ir}) of the insulating phase cannot be substituted into the expressions given below, but should be obtainable by fitting the results.

2.1. Matrix media

In matrix media, the conductivity results are often presented using both the complex impedance (Z^*) and modulus (M^*) representations. The notations adopted for Z^* and M^* are $Z^* = Z' - iZ''$ and $M^* = M' + iM''$, where $M^* = i\omega Z^*$, and Z' and Z'' are the real and imaginary impedances, respectively, while M' and M'' are the corresponding modulus parameters. This leads to the following equations:

$$M' = \omega Z'', \qquad M'' = \omega Z'. \tag{1}$$

Note that the results are often presented as complex plane (Nyquist) plots ($Z'' - Z'$ and $M'' - M'$) or Z''-frequency and M''-frequency plots. When the more conducting phase forms the "dominant" matrix, these plots show only a single arc—the peak frequency of which is determined by the properties of the components and the volume fraction of each [24]. When the insulating phase forms the matrix, there are two arcs, each characterizing the contribution of one component. The peak frequencies for the multiple component arc (above φ_c) and the two single component arcs (below φ_c) are given by

$$\begin{aligned} f_p &= \frac{\sigma_{mr}(\varphi,0)}{2\pi\varepsilon_0\varepsilon_{mr}(\varphi,0)} \quad (\varphi < \varphi_c), \\ f_p &= \frac{\sigma_{cr}(0)}{2\pi\varepsilon_0\varepsilon_{cr}(0)} \quad (\varphi < \varphi_c; \text{ high frequency}), \\ f_p &= \frac{\sigma_{ir}(0)}{2\pi\varepsilon_0\varepsilon_{ir}(0)} \quad (\varphi < \varphi_c; \text{ low frequency}), \end{aligned} \tag{2}$$

respectively. The subscript "m" refers to the properties of the composite, and "c" and "i" to those of the components. The $\varepsilon_{xr}(0)$ are the static dielectric constants. Above φ_c, the peak frequency (ω_p) increases with φ. Note that in order to observe all these arcs, the experimental apparatus must adequately cover all ω values defined by (2).

The MW/HS equations ([2] and the references therein), derived directly from Maxwell's equations, for the spherical isotropic microstructure shown in Figure 1, are

$$\frac{\sigma_m - \sigma_c}{\sigma_m + 2\sigma_c} = \frac{(1-\varphi)(\sigma_i - \sigma_c)}{\sigma_i + 2\sigma_c}, \tag{3a}$$

$$\frac{\sigma_m - \sigma_i}{\sigma_m + 2\sigma_i} = \frac{\varphi(\sigma_c - \sigma_i)}{\sigma_c + 2\sigma_i}. \tag{3b}$$

The MW/HS media can be visualized as built up out of a space-filling array of coated spheres, with an infinite range of sizes, as illustrated in Figure 1. In (3a), σ_c is the conductivity of the coating or matrix material, while σ_i is the conductivity of the spherical core. In (3b), σ_c is for the core while σ_i is for the coating (matrix). Note that the model has been widely and successfully applied to systems which differ from the idealized microstructures shown in Figure 1, for instance, the electrical conductivity results and the complex impedance plane plots for sintered polycrystalline yttria stabilized zirconia. With values of φ close to one ($\varphi \approx 0.999$), micron-sized grains (σ_c), and grain boundaries (σ_i), a few nanometers thick (3b) and the BLM are found to successfully fit experimental data provided that suitable dispersive expressions are substituted for $\sigma_c(\omega)$ and $\sigma_i(\omega)$ [25]. Suitable dispersive expressions include the universal dielectric response function [26] and an expression due to León et al. [27].

Other effective media theories are discussed in the feature article by McLachlan et al. [2] and the review article by Meredith and Tobias [28] which gives expressions for the electrical conductivity for a wide variety of other structures.

2.2. Percolation media: critical volume fraction

If conducting spheres (discs), of just sufficient size to touch their nearest neighbors, are placed at random on the sites of 3D (2D) Bravais lattices, it is found that φ_c is 0.16 ± 0.02 (0.50 ± 0.02) [2, 29]. If equally sized conducting and nonconducting spheres are placed at random in a container, φ_c is also

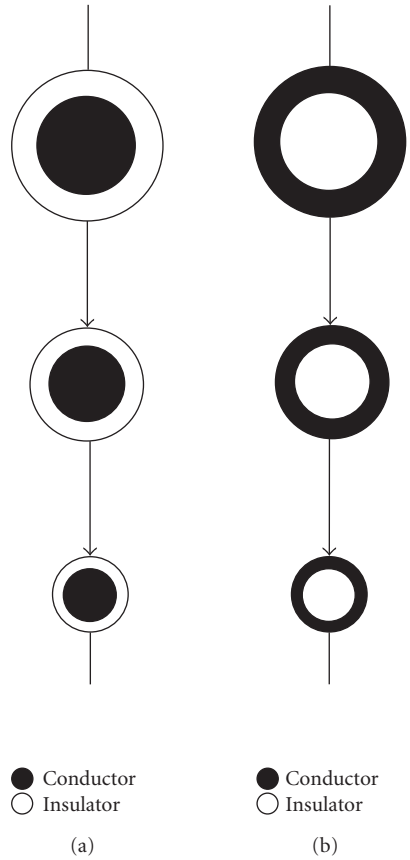

Figure 1: The microstructure described by the (a) insulator-host and (b) conductor-host Maxwell-Wagner effective media (MW/HS) theory.

found to be about 0.16. This value of φ_c is often taken to characterize 3D random media but other values of φ_c are permitted [2, 21, 29]. The case, where $\varphi_c > 0.16$, is best illustrated using the grain consolidation model illustrated in Figures 2(a) and 2(b). The model starts with the random nucleation of conducting (white) spheres which grow to form a random close-packed lattice of touching spheres at $\varphi = 0.636$. As the radii of the spheres increase further, the interfacial contact area grows, as illustrated in Figure 2(b), which shows thin layers of insulating material between all the conducting grains. Examining Figure 2(b) shows that the sample becomes conducting when a sufficient number of the barriers, between the conducting grains, have been removed at random for a percolation path to form, which, for thin barriers, can give a high value of φ_c. In the case of nanostructures, the barriers will almost certainly be below the tunneling length so that a conducting critical path, which passes through a series of sufficiently low tunnel barriers, will be formed at φ_c. Below φ_c, the electrons follow a "pseudopercolation" path through a series of barriers with the lowest resistances.

For $\varphi_c < 0.16$, three models can be considered. The first is the grain consolidation model illustrated in Figures 2(c) and 2(d), where insulating spheres have now nucleated and grown sufficiently to confine the conducting material (white) to intergranular channels (see Figure 2(c)). At a φ value of 0.03 (φ_c), the channels become isolated. In the sintering of ceramics, it is well known that closed porosity is usually achieved at a value of about 3%. The next model is for cellular structures, which is illustrated in Figure 3. Here, a fine conducting powder has been compacted with a coarse insulating one. Calculations, based on there being a percolation path on the surface of the insulating spheres, have been made by Kusy [30]. For instance, when the ratio of the radii of the components is 30, $\varphi_c \approx 0.03$. A series of such cellular systems, which give φ_c's between 0.012 and 0.065, has been examined in Chiteme and McLachlan [12]. For particles with irregular geometries, especially extended ones (rods, discs), one must use the excluded volume model of Balberg et al. [31]. This has been used in explaining the results for single and multiple wall carbon nanotubes (SWCNT and MWCNT), modeled as random sticks in 3D (McLachlan et al. [22] and the references therein). Figure 4 shows random sticks in 2D and Figure 5 shows φ_c as a function of the aspect ratio of the sticks. According to Figure 5, the SWCNT bundles should have a φ_c higher than that observed [22]. Reasons for this are given by McLachlan et al. [22].

2.3. Percolation media: the TEPPE and experimental results

Note that no experimental details will be given here; for these the reader should consult the original papers. As previously stated, a recent series of papers [7–13, 16, 32] has shown that the TEPPE, which is

$$(1-\varphi)\frac{\sigma_i^{1/s}-\sigma_m^{1/s}}{\sigma_i^{1/s}+A\sigma_m^{1/s}}+\varphi\frac{\sigma_c^{1/t}-\sigma_m^{1/t}}{\sigma_c^{1/t}+A\sigma_m^{1/t}}=0, \tag{4}$$

with $A = (1-\varphi_c)/\varphi_c$ and the exponents s and t, best describes experimental results for percolation systems, especially the second-order terms [10, 11]. When $s = t = 1$ and $\varphi_c = 1/3$, the equation is equivalent to the Bruggeman symmetric media equation [2, 21]. Equation (4) yields the two limits

$$|\sigma_c| \longrightarrow \infty : \sigma_m = \sigma_i\left(\frac{\varphi_c}{\varphi_c-\varphi}\right)^s \quad \text{or} \quad \varepsilon_{mr} = \varepsilon_{ir}\left(\frac{\varphi_c}{\varphi_c-\varphi}\right)^s, \quad \varphi < \varphi_c, \tag{5}$$

$$|\sigma_i| \longrightarrow 0 : \sigma_m = \sigma_c\left(\frac{\varphi-\varphi_c}{1-\varphi_c}\right)^t \quad \text{or} \quad \varepsilon_{mr} = \varepsilon_{ir}\left(\frac{\varphi-\varphi_c}{1-\varphi_c}\right)^t, \quad \varphi > \varphi_c. \tag{6}$$

These equations are the normalized standard percolation results [18, 19] and characterize the exponents s and t.

In the crossover region, where $\varphi \cong \varphi_c$, and which lies between

$$\varphi_c - \left(\frac{\sigma_i}{\sigma_c}\right)^{1/t+s} \quad \text{or} \quad \left(\varphi_c - \frac{\omega\varepsilon_0\varepsilon_{ir}}{\sigma_{cr}}\right)^{1/t+s} < \varphi < \varphi_c + \left(\frac{\sigma_i}{\sigma_c}\right)^{1/t+s} \quad \text{or} \quad \left(\varphi_c + \frac{\omega\varepsilon_0\varepsilon_{ir}}{\sigma_{cr}}\right)^{1/t+s}, \tag{7}$$

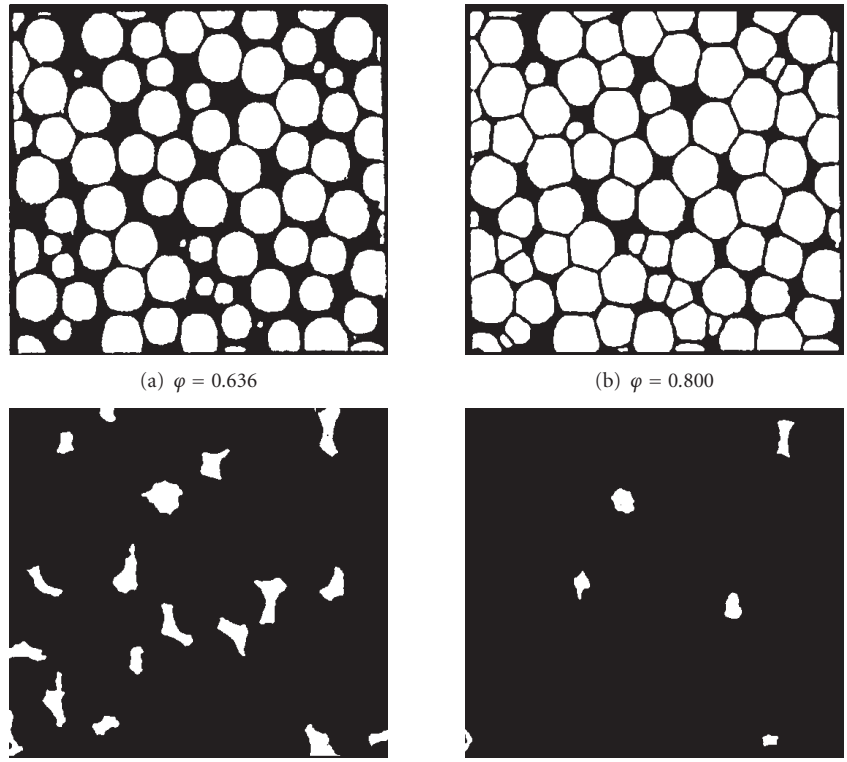

(a) $\varphi = 0.636$ (b) $\varphi = 0.800$

(c) $\varphi = 0.10$ (d) $\varphi = 0.03$

Figure 2: The grain consolidation model.

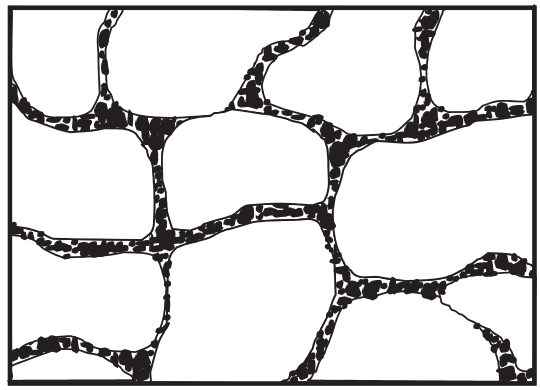

Figure 3: Cellular micro-/nanostructure. $\varphi_c = 0.03$, for a radius ratio of about 30.

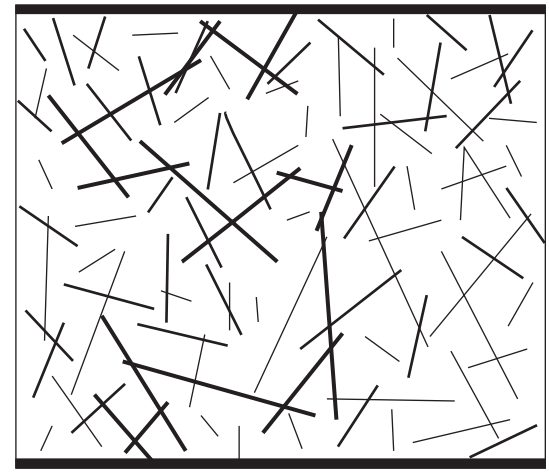

Figure 4: Percolation network of random sticks in two dimensions.

(4) gives

$$\sigma_m \approx \sigma_i^{t/(s+t)} \sigma_c^{s/(s+t)} \quad \text{or} \quad \left((\omega \varepsilon_0 \varepsilon_{ir})^{t/(s+t)} \sigma_{cr}^{s/(s+t)} \right), \quad (8)$$

which is in agreement with the theory given in Clerc et al. [18] and Bergman and Stroud [19]. Equation (8) shows that, in the crossover region, the conductivity σ_{mr} should be proportional to $\omega^{t/(s+t)}$ and the dielectric constant ε_{mr} (recall that $\varepsilon_{xy} = \sigma_{xy}/\omega\varepsilon_0$) is proportional to $\omega^{s/(s+t)}$. Note that (5) and (6) are not valid in the crossover region.

The relationship between the DC exponents, s and t, and the high frequency slopes, $u_t = t/(s+t), v_t = s/(s+t)$ and $u_t + v_t = 1$, in the crossover region, is a basic premise for universal behavior, upon which the three standard percolation equations are based ([18–20] and the references therein). In this respect, all AC experimental results ([7–13, 16] and the

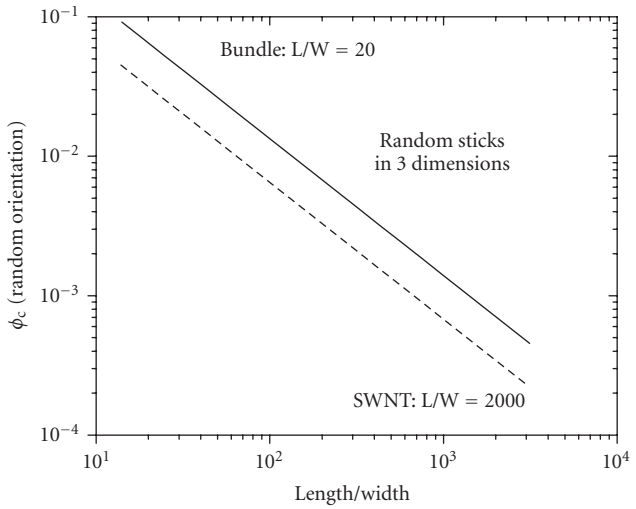

Figure 5: The percolation thresholds for random sticks.

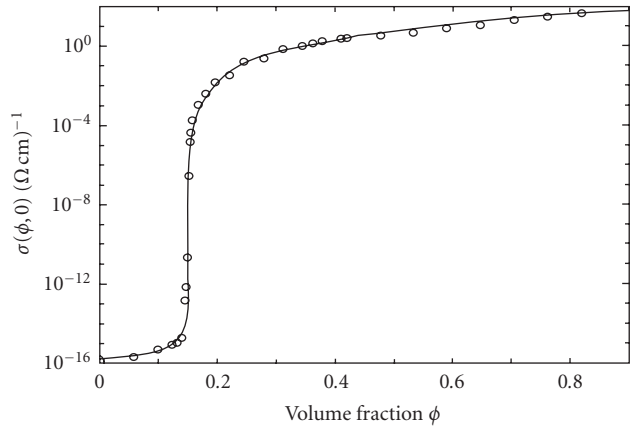

Figure 6: DC percolation results for Graphite-hBN discs. $\varphi_c = 0.150 \pm 0.001$, $s = 1.01 \pm 0.05$, and $t = 2.63 \pm 0.07$.

references therein) are nonuniversal, with the results in Wu and McLachlan [7, 8] being the closest to universal. Therefore, these results are used to illustrate the first-order results, σ_{mr} above φ_c and ε_{mr} below φ_c, and the second-order results, ε_{mr} above φ_c and σ_{mr} below φ_c. Arguably, the best DC conductivity results, for a percolation system, are those measured on compressed Graphite-hBN discs, which are given in Figure 6, from which φ_c, s, and t can easily be determined using (4). Figure 7 shows the AC conductivity plotted as a function of frequency for a loosely packed Graphite-hBN mixture, and Figure 8 shows the dielectric constant as a function of frequency. These results are presented as they are the only ones where the results below φ_c can be scaled. Note how one can clearly distinguish between samples above and below φ_c in Figure 7. Close to φ_c, the slope in the high-frequency region for a percolation system should be $t/(s+t)$ with s and t being determined from the DC results. Not too much can be determined about the dielectric constant from these plots, except that the linear slope, which should be $s/(s+t)$, is only observed for higher frequencies and very close to φ_c, as it is to be expected from (5). Universality requires that the experimental slopes of such plots be $u_e = t/(s+t)$ and $v_e = s/(s+t)$, using the s and t determined from DC measurements. Note that whereas the slopes in the graphite boron nitride system are close to the universal values, in most systems they are not [12, 16] and $u_e + v_e < 1$. The dielectric constant results shown in Figure 8 are not even qualitatively in accordance with the predictions of the standard equations. Results of this nature can be qualitatively fitted using (4) [10]. However, a more complex algorithm is needed for quantitative fitting [11]. Note that the dielectric constant is frequency dependant below φ_c [12]—something which has never been previously taken into account theoretically, using (4) or any other expression.

Figure 9 shows a further plot of the conductivity as a function of frequency, from a special experiment using loosely packed Graphite-hBN in ultra dry air [10]. The contributions to the conductivity from the insulator (DC and

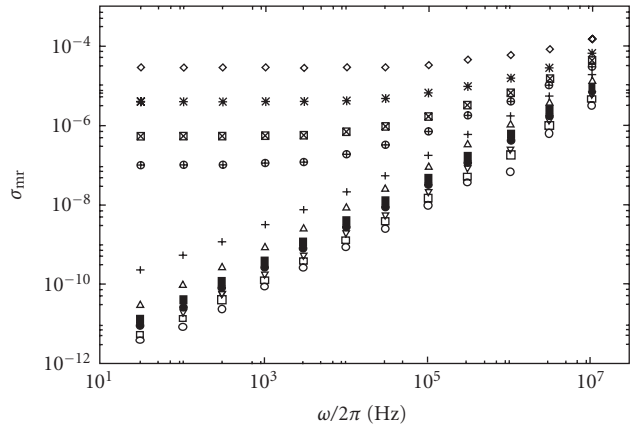

Figure 7: AC conductivity plotted against frequency for a loosely packed Graphite-hBN mixture. The range of φ values is between 0.112 and 0.133. A gap occurs between the low-frequency results above and below φ_c.

dielectric loss) and the percolation clusters and their sum are shown by the solid line in the figure (see Wu and McLachlan [8] for further details). To date, the percolation contribution has been only clearly seen in this system, where the insulator is mainly dry air and a little dry BN. In most systems, the percolation contribution is swamped by the contribution from σ_{ii}.

2.4. The exponents s and t

The universal value of the exponent t (t_{un}), which is usually observed in computer simulations and for "ideal" systems, is 2 [18, 19] while $s_{un} \approx 0.87$. However, values in the ranges of $0.37 < s < 1.28$ and $1 < t < 6.27$ can be found in the literature ([15] and the references therein). Kogut and Straley [33] showed, in computer simulations, that if the low-conductance bonds in the percolation network, or the

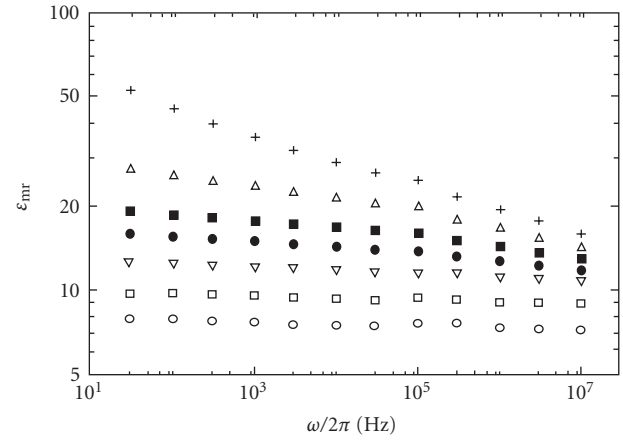

Figure 8: Dielectric constant plotted against frequency for a loosely packed Graphite-hBN mixture. The range of φ values is between 0.112 and 0.123. The top curve is for a sample marginally above φ_c.

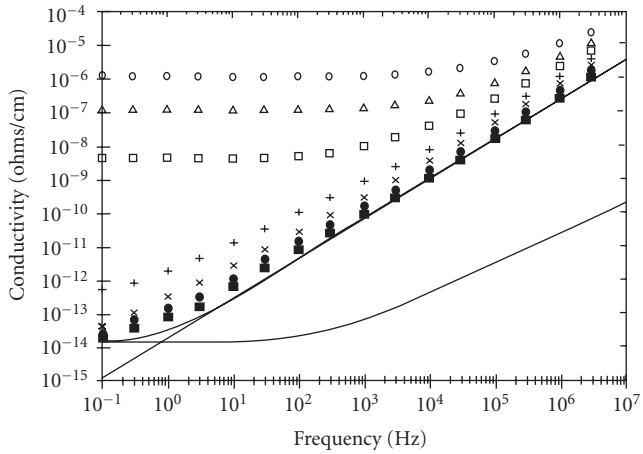

Figure 9: AC conductivity of loosely packed Graphite-hBN in ultra dry air. The straight line is the calculated contribution from the percolation clusters and the lowest plot shows the total dielectric loss.

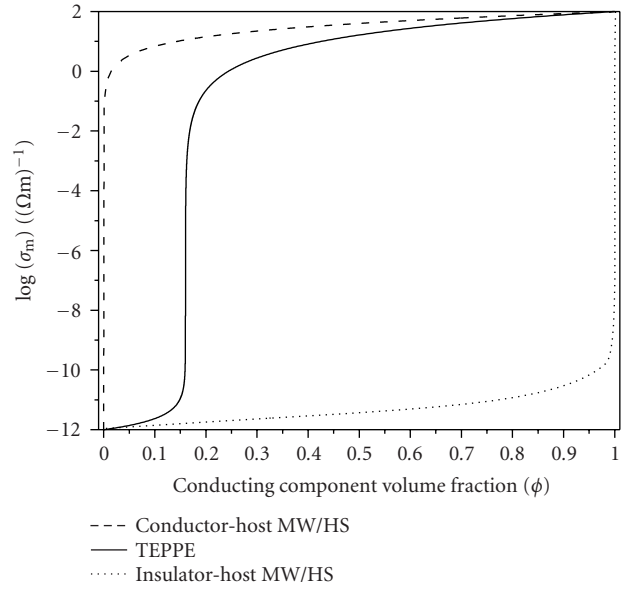

Figure 10: DC conductivities for the conductor-host Maxwell-Wagner/Hashin-Shtrikman equation, the TEPPE, and the insulator-host Maxwell-Wagner/Hashin-Shtrikman equation. In the simulation, $\sigma_{cr} = 10^2(\Omega m)^{-1}$ and $\sigma_{ir} = 10^{-12}(\Omega m)^{-1}$. For the TEPPE, $\varphi_c = 0.16$, $s = 0.87$, and $t = 2$.

intergranular conductances of the conducting component in a continuum system, have a very wide distribution, then t can be larger than t_{un}. This distribution can be due to a large range of effective geometrical resistivity factors in a continuous homogeneous conducting phase, as occurred in the Swiss Cheese (random void (RV)) model and the inverse Swiss Cheese (inverse random void (IRV)) model [32, 34]. In the Swiss Cheese model, a range of very thin and highly resistive threads of the conductor (Cheese), between the large overlapping voids (air), give rise to a wide distribution in the conductances between the more extended or bulky regions of conductor. These models give values for t in the range of 2–2.5. An extension to the RV model allowing still higher (apparently unlimited) values of t is given berg [35]. The links, blobs, and nodes model [36, 37] gives an upper limit of 2.35. Note that all of the above models assume a homogeneous (nongranular) conducting phase. A model for granular conducting systems which gives rise to $t > t_{un}$ was proposed by Balberg [38]. This model is based on the dominant resistances in the current carrying links and blobs (now consisting of a granular conductor) being due to a large range of interparticle tunneling contacts. Due to the characteristic dimensions of nanostructures, the intergranular distances will often be 10 nm thick or less, that is, below the characteristic tunneling distance. This means that the Balberg [38] model will probably be the most appropriate for nanostructures, where values of t greater than two are to be expected.

One might expect the charging effect or coulomb blockage in nanostructures because, for a 100 nm radius (R) sphere carrying charge of one excess electron, the charging energy, which is e^2/C or $e^2/2\pi\varepsilon_0 R$, is equal to the thermal energy kT at 300 K. However, this will not affect the conductivity of a bulk sample because, well below φ_c, there will be a large number of hopping conductivity paths, with a number of different hopping lengths in each. This, combined with the fact that e^2/C will vary from site to site, will average out any observable effects. Closer to φ_c, the hopping occurs between random clusters which have larger and more varied C values, which will again lead to a smearing out of charging effects. It should also be noted that it has been shown by McLachlan et al. [13] that the scaling results for percolation systems and universal conductivity systems, which have been observed in amorphous conductors, ionic conductors, lightly doped semiconductors, and other disordered systems, are very similar. As in some, but not all, universal conductivity systems, coulomb blocking occurs; the presence of coulomb blocking does not necessarily invalidate the TEPPE.

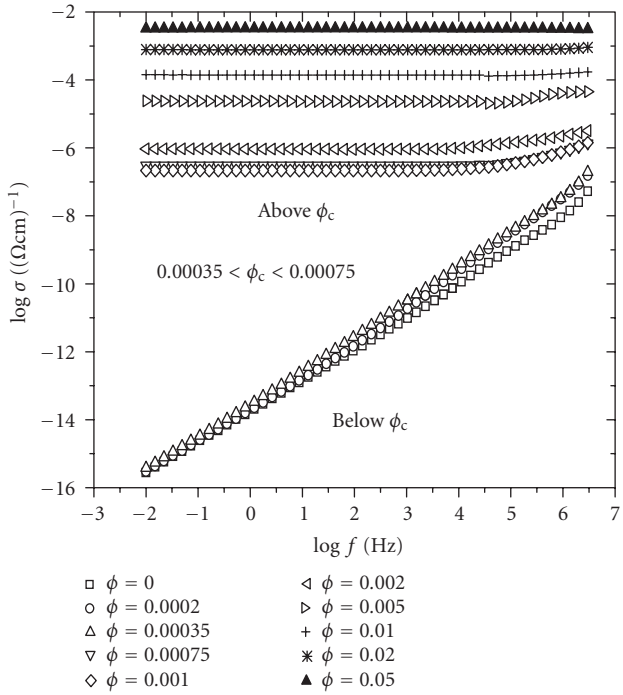

FIGURE 11: The AC conductivity of SWCNT-polymer composites at various φ values. Note the big jump in the conductivity around φ_c [22].

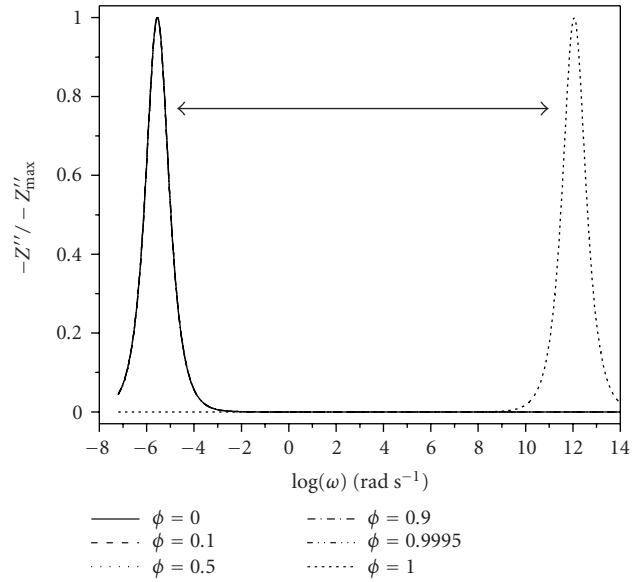

FIGURE 12: The normalized impedance for an insulator-host Maxwell-Wagner/Hashin-Shtrikman system. For the ratio of component conductivities in the simulations, no peaks are observed between those of the insulating and conducting components. The system is dominated either by the insulating or the conducting component. For the simulations, $\sigma_{cr} = 10^2(\Omega m)^{-1}$, $\varepsilon_{cr} = 10$, $\sigma_{ir} = 10^{-16}$, and $\varepsilon_{ir} = 4$ (For lower values of σ_{cr}/σ_{ir} two peaks are observed in the spectrum).

3. DIFFERENTIATING BETWEEN A MATRIX AND A PERCOLATION NANOSTRUCTURE

Fully fitting DC conductivity measurements, over a wide range of compositions, is the easiest and clearest way of distinguishing nanostructures. Figure 10 shows the DC conductivities for the conductor-host MW/HS equation, TEPPE, and the insulator-host MW/HS equation. It can be clearly seen that over a wide enough range of φ's (on either side of φ_c for the percolation system), the three models predict vastly different conductivities.

Equally good, but involving far more work, is a full fit of the AC conductivity data. Youngs [14, 15] describes the use of a genetic algorithm that enables robust fitting of AC conductivity data to the TEPPE (GEM). With sufficient care, and the use of both the AC and DC data, satisfactory results can be obtained, from the TEPPE, for systems with data only on one side of φ_c [39][1]. Various algorithms can be used to fit data to the MW/HS equations [25, 39]. Unfortunately, it is not possible to differentiate between the different nanostructures from features of the AC conductivity data, such as the high frequency slope of the conductivity-frequency curves, for a sample of a single composition. These features are influenced not only by the structure of the composites, but also by the dispersive properties of their components [25].

Where AC conductivity data are available for various compositions, there are various ways of distinguishing between percolation and effective media systems. Percolation and effective media systems can be differentiated by the big changes (usually several orders of magnitude) that occur in the AC conductivities at φ_c for the percolation system. Figure 11 shows the AC conductivities, at various φ's for a SWCNT-polymer composite. The samples clearly lie in two groups: one below the percolation threshold and another above. Such a big jump in the AC conductivity, for a relatively small change in φ, is not observed for effective media systems, except where $\varphi \approx 0$ or 1.

The changes in the positioning of peaks in Z''-frequency (or $Z' - Z''$) plots can also be used to distinguish between systems described by the different models. For the insulator-host MW/HS, the position of the impedance peak does not change much with increasing φ but instead remains under or very close to the $\varphi = 0$ peak, until $\varphi \approx 1$, as shown in Figure 12.

For a system described by the conductor-host MW/HS, the peaks in Z'', as shown in Figure 13, remain close to the $\varphi = 1$ peak until $\varphi \approx 0$.

For a percolation system, Z'' peaks are seen at all frequencies between the characteristic frequencies of the components as shown in Figure 14. Up to φ_c, the impedance is dominated by the insulating component and the Z'' peaks

[1] Copies of the fitting and simulation algorithms implemented in MATHEMATICA can be obtained from G. S.

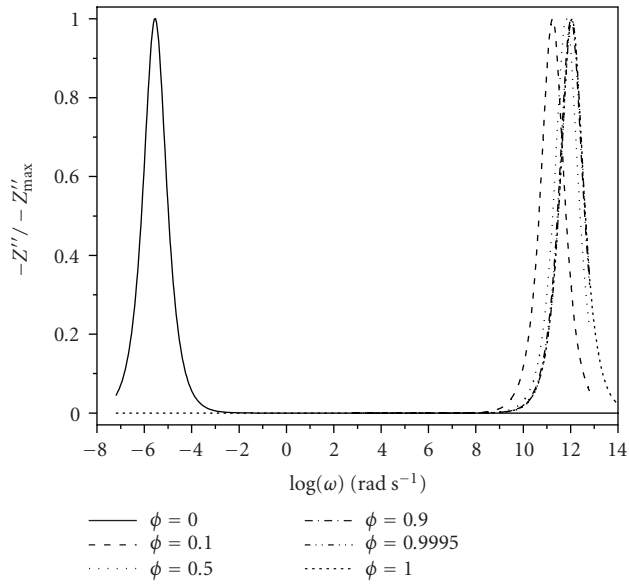

Figure 13: Normalized impedance for the conductor-host Maxwell-Wagner/Hashin-Shtrikman model. Note that the single peak starts close to the $\varphi = 1$ peak, even for very low φ and moves to the right, closer to $\varphi = 1$ with increasing φ. For the simulations, $\sigma_{cr} = 10^2(\Omega m)^{-1}$, $\varepsilon_{cr} = 10$, $\sigma_{ir} = 10^{-16}(\Omega m)^{-1}$, and $\varepsilon_{ir} = 4$.

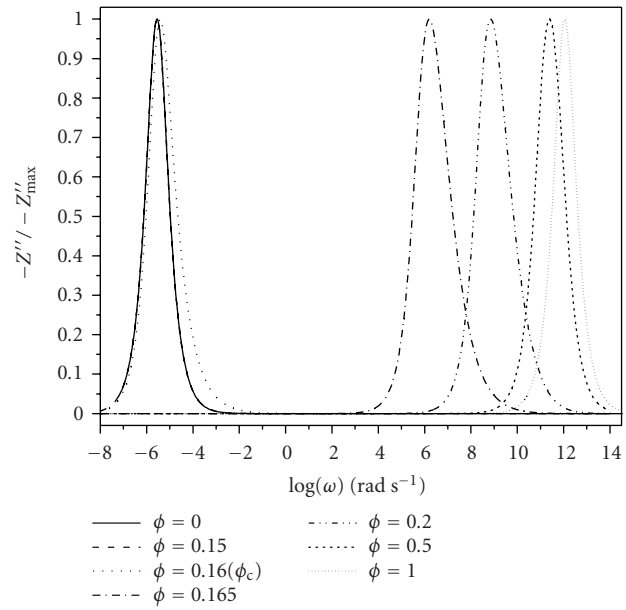

Figure 14: The normalized impedance for a percolation system. Note the peaks at frequencies in between those of the insulating and conducting components. For the simulations, $\sigma_{cr} = 10^2(\Omega m)^{-1}$, $\varepsilon_{cr} = 10$, $\sigma_{ir} = 10^{-16}(\Omega m)^{-1}$, $\varepsilon_{ir} = 4$, $s = 1$, $t = 2$, and $\varphi_c = 0.16$.

are all superimposed onto the $\varphi = 0$ peak. However, just above φ_c, the peak starts to move towards the $\varphi = 1$ peak with increasing φ.

Similar behavior as seen in Figures 12, 13, and 14 is observed for smaller σ_i/σ_c with the only difference being that the insulator and conductor peaks lie closer together. If $\sigma_i/\sigma_c > 10^{-3}$, the peaks will start to overlap which may cause problems.

4. CONCLUSIONS

This paper has shown how the AC and DC conductivity (dielectric constant) results, for binary composites, with one or more of which having nanodimensions, can be analyzed in terms of either (i) a matrix structure using the Maxwell-Wagner/Hashin-Shtrikman (or Bricklayer) model or (ii) a percolation structure using the two-exponent phenomenological percolation equation (TEPPE). It is also shown how the two structures may be distinguished using electrical measurements. As the actual complex conductivities appear in expressions, it is theoretically possible to determine the dispersive conductivities for both components and, for percolation systems, the critical volume fraction as well as the exponents s and t. Unfortunately, even when a large amount of data, on both sides of the critical volume fraction, are available, this is a formidable task due to the large number of unknown parameters (a dispersive medium has to have two or more). In practice, it will probably be necessary to know an expression to directly measure the conductivity of one of the components. If only one component is nanosized, it should be possible to deduce its dispersive conductivity by fitting the results for the composite using the MW/HS equations or the TEPPE together with the best expressions for the dispersive conductivity of the other component.

REFERENCES

[1] Z. Hashin and S. Shtrikman, "A variational approach to the theory of the effective magnetic permeability of multiphase materials," *Journal of Applied Physics*, vol. 33, no. 10, pp. 3125–3131, 1962.

[2] D. S. McLachlan, M. Blaszkiewicz, and R. E. Newnham, "Electrical resistivity of composites," *Journal of the American Ceramic Society*, vol. 73, no. 8, pp. 2187–2203, 1990.

[3] M. Campo, L. Woo, T. Mason, and E. Garboczi, "Frequency-dependent electrical mixing law behavior in spherical particle composites," *Journal of Electroceramics*, vol. 9, no. 1, pp. 49–56, 2002.

[4] J.-H. Hwang, D. S. Mclachlan, and T. O. Mason, "Brick layer model analysis of nanoscale-to-microscale cerium dioxide," *Journal of Electroceramics*, vol. 3, no. 1, pp. 7–16, 1999.

[5] D. S. McLachlan, C. Chiteme, W. D. Heiss, and J. Wu, "The correct modelling of the second order terms of the complex AC conductivity results for continuum percolation media, using a single phenomenological equation," *Physica B*, vol. 338, no. 1–4, pp. 256–260, 2003.

[6] D. S. McLachlan, C. Chiteme, W. D. Heiss, and J. Wu, "Fitting the DC conductivity and first order AC conductivity results for continuum percolation media, using percolation theory and a single phenomenological equation," *Physica B*, vol. 338, no. 1–4, pp. 261–265, 2003.

[7] J. Wu and D. S. McLachlan, "Percolation exponents and thresholds obtained from the nearly ideal continuum

percolation system graphite-boron nitride," *Physical Review B*, vol. 56, no. 3, pp. 1236–1248, 1997.

[8] J. Wu and D. S. McLachlan, "Scaling behaviour of the complex conductivity of graphite-boron nitride systems," *Journal of Physical Review B*, vol. 58, no. 22, pp. 14880–14887, 1998.

[9] D. S. McLachlan and M. B. Heaney, "Complex ac conductivity of a carbon black composite as a function of frequency, composition, and temperature," *Physical Review B*, vol. 60, no. 18, pp. 12746–12751, 1999.

[10] D. S. McLachlan, W. D. Heiss, C. Chiteme, and J. Wu, "Analytic scaling functions applicable to dispersion measurements in percolative metal-insulator systems," *Physical Review B*, vol. 58, no. 20, pp. 13558–13564, 1998.

[11] W. D. Heiss, D. S. McLachlan, and C. Chiteme, "Higher-order effects in the dielectric constant of percolative metal-insulator systems above the critical point," *Physical Review B*, vol. 62, no. 7, pp. 4196–4199, 2000.

[12] C. Chiteme and D. S. McLachlan, "AC and DC conductivity, magnetoresistance, and scaling in cellular percolation systems," *Physical Review B*, vol. 67, no. 2, Article ID 024206, 18 pages, 2003.

[13] D. S. McLachlan, G. Sauti, and C. Chiteme, "Static dielectric function and scaling of the ac conductivity for universal and nonuniversal percolation systems," *Physical Review B*, vol. 76, no. 1, Article ID 014201, 13 pages, 2007.

[14] I. J. Youngs, *Electrical percolation and the design of functional electromagnetic materials*, Ph.D. thesis, Electronic and Electrical Engineering, University College, London, UK, 2001.

[15] I. J. Youngs, "Exploring the universal nature of electrical percolation exponents by genetic algorithm fitting with general effective medium theory," *Journal of Physics D*, vol. 35, no. 23, pp. 3127–3137, 2002.

[16] C. Chiteme, D. S. McLachlan, and G. Sauti, "AC and DC percolative conductivity of magnetite-cellulose acetate composites," *Physical Review B*, vol. 75, no. 9, Article ID 094202, 13 pages, 2007.

[17] C. Brosseau, "Generalized effective medium theory and dielectric relaxation in particle-filled polymeric resins," *Journal of Applied Physics*, vol. 91, no. 5, pp. 3197–3204, 2002.

[18] J. P. Clerc, G. Giraud, J. M. Laugier, and J. M. Luck, "The electrical conductivity of binary disordered systems, percolation clusters, fractals and related models," *Advances in Physics*, vol. 39, no. 3, pp. 191–309, 1990.

[19] D. J. Bergman and D. Stroud, "The physical properties of macroscopically inhomogeneous media," *Solid State Physics*, vol. 46, pp. 148–270, 1992.

[20] C.-W. Nan, "Physics of inhomogeneous inorganic materials," *Progress in Materials Science*, vol. 37, pp. 1–116, 1993.

[21] D. S. Mclachlan, "Analytical functions for the DC and AC conductivity of conductor-insulator composites," *Journal of Electroceramics*, vol. 5, no. 2, pp. 93–110, 2000.

[22] D. S. McLachlan, C. Chiteme, C. Park, et al., "AC and DC percolative conductivity of single wall carbon nanotube polymer composites," *Journal of Polymer Science Part B*, vol. 43, no. 22, pp. 3273–3287, 2005.

[23] D. S. McLachlan, R. Rosenbaum, A. Albers, et al., "The temperature and volume fraction dependence of the resistivity of granular Al-Ge near the percolation threshold," *Journal of Physics: Condensed Matter*, vol. 5, no. 27, pp. 4829–4842, 1993.

[24] D. S. McLachlan, J.-H. Hwang, and T. O. Mason, "Evaluating dielectric impedance spectra using effective media theories," *Journal of Electroceramics*, vol. 5, no. 1, pp. 37–51, 2000.

[25] G. Sauti, *Electrical Conductivity and Permittivity of Ceramics and other Composites*, Ph.D. thesis, Physics, University of the Witwatersrand, Johannesburg, South Africa, 2005.

[26] A. K. Jonscher, "The 'universal' dielectric response," *Nature*, vol. 267, no. 5613, pp. 673–679, 1977.

[27] C. León, M. L. Lucía, and J. Santamaría, "Correlated ion hopping in single-crystal yttria-stabilized zirconia," *Physical Review B*, vol. 55, no. 2, pp. 882–887, 1997.

[28] R. E. Meredith and C. W. Tobias, "Conduction in heterogenous systems," in *Advances in Electrochemistry and Electrochemical Engineering*, C. Tobias, Ed., vol. 2, pp. 15–47, John Wiley & Sons, New York, NY, USA, 1962.

[29] R. Zallen, *The Physics of Amorphous Solids*, John Wiley & Sons, New York, NY, USA, 1983.

[30] R. P. Kusy, "Influence of particle size ratio on the continuity of aggregates," *Journal of Applied Physics*, vol. 48, no. 12, pp. 5301–5305, 1977.

[31] I. Balberg, C. H. Anderson, S. Alexander, and N. Wagner, "Excluded volume and its relation to the onset of percolation," *Physical Review B*, vol. 30, no. 7, pp. 3933–3943, 1984.

[32] B. I. Halperin, S. Feng, and P. N. Sen, "Differences between Lattice and continuum percolation transport exponents," *Physical Review Letters*, vol. 54, no. 22, pp. 2391–2394, 1985.

[33] P. M. Kogut and J. P. Straley, "Distribution-induced nonuniversality of the percolation conductivity exponents," *Journal of Physics C*, vol. 12, no. 11, pp. 2151–2159, 1979.

[34] S. Feng, B. I. Halperin, and P. N. Sen, "Transport properties of continuum systems near the percolation threshold," *Physical Review B*, vol. 35, no. 1, pp. 197–214, 1987.

[35] I. Balberg, "Limits on the continuum-percolation transport exponents," *Physical Review B*, vol. 57, no. 21, pp. 13351–13354, 1998.

[36] H. E. Stanley, "Cluster shapes at the percolation threshold: and effective cluster dimensionality and its connection with critical-point exponents," *Journal of Physics A*, vol. 10, no. 11, pp. L211–L220, 1977.

[37] A. Coniglio, "Cluster structure near the percolation threshold," *Journal of Physics A*, vol. 15, no. 12, pp. 3829–3844, 1982.

[38] I. Balberg, "Tunneling and nonuniversal conductivity in composite materials," *Physical Review Letters*, vol. 59, no. 12, pp. 1305–1308, 1987.

[39] G. Sauti and D. S. McLachlan, "Impedance and modulus spectra of the percolation system silicon-polyester resin and their analysis using the two exponent phenomenological percolation equation," *Journal of Materials Science*, vol. 42, no. 16, pp. 6477–6488, 2007.